

STRANDS VERSUS BARS FOR POSITIVE MOMENT CONNECTION OF PCBT GIRDERS

Charles D. Newhouse, Ph.D., P.E., Dept. of Civil Engineering, Texas Tech University, Lubbock, TX

Carin L. Roberts-Wollmann, Ph.D., P.E., Dept. of Civil and Environmental Engineering, Virginia Tech, Blacksburg, VA

Thomas E. Cousins, Ph.D., P.E., Dept. of Civil and Environmental Engineering, Virginia Tech, Blacksburg, VA

Rodney T. Davis, Ph.D., P.E., Virginia Transportation Research Council, Charlottesville, VA

ABSTRACT

There are many benefits to connecting concrete girders over an interior support. A simple approach to connecting the girders uses longitudinal steel in the deck to resist the tensile force due to negative moment. For positive moment caused by secondary effects (creep, shrinkage, thermal gradients), the tensile force at the bottom of the connection is often resisted by extending either strands or bars from the ends of the girders and casting them within a continuity diaphragm. This study compares the performance of two different positive moment connections that are commonly used, one with extended 1/2 in. (14.7 mm) diameter prestressing strands bent at 90 degrees and the other with extended 180 degree bent No. 6 (19M) reinforcing bars. Full depth PCBT (Precast Concrete Bulb Tee) 45 in. (1143 mm) deep sections were made continuous by casting a continuity diaphragm and a conventionally reinforced deck. The two span systems were tested to determine the initial positive cracking moments, integrity of the connections under cyclic loads, and ultimate positive moment capacities. When subjected to similar loading conditions, the connection made with the mild reinforcing bars performed better than the connection made with the prestressing strands.

Keywords: Continuity Diaphragm, Restraint Moment, Cracking Moment, Ultimate Capacity

INTRODUCTION

Many long term benefits can be achieved when a joint is eliminated by connecting simple span girders with a continuity diaphragm and a continuous deck. These benefits have been recognized since the late 1950's in the United States.¹ The reduced potential for corrosion by keeping deicing salts off of the bearings and the ends of the girders is often reason enough to design a structure continuous. In addition, the traveling public prefers the smoother ride that results when joints are eliminated. Structurally, connecting the girders together adds redundancy to the system, which is invaluable in an overload event such as an earthquake, a vehicular impact, or a flood.

Although there are many benefits to making simple span girders continuous, doing so introduces complexity to the design and analysis of the structural system. Once the girders are made continuous with the continuity connection, time dependent changes due to creep and shrinkage cause end rotations to develop over the continuous supports. Since these end rotations are restrained by the continuity connection, restraint moments develop. Conventional analysis is often used to determine the negative restraint moments due to live loads and superimposed dead loads. To determine the positive restraint moments, design methods such as the PCA Method² and the program RMCalc³ have been widely used. In addition to time dependent restraint moments, it has been shown that thermal gradients can also cause significant positive restraint moments.^{4,5}

According to a recent survey, slightly over half of the respondents that use a positive moment connection use extended prestressing strands while the remaining use some type of extended reinforcing steel.⁶ Typically, the extended strand or the extended reinforcing steel is bent up at a 90 degree angle and cast within the continuity diaphragm. Only approximately 7 percent of the respondents indicated that they used an alternate type of connection such as mechanical strand connectors or welding the bars together to produce the connection.

OBJECTIVE

The objective of this study was to compare the performance of two positive moment connections, one made with extended strands and the other made with extended reinforcing steel. Both connections were subjected to the same loading regimen so that their performances could be compared. First, the connections were subjected to slowly applied positive moments to determine the positive moment that would cause initial cracking at the bottom of the interface of the continuity diaphragm and the end of the girder. Next, the connections were subjected to 10,000 moment cycles designed to simulate the anticipated positive thermal cycles a typical structure would encounter in a 75 year service life. Finally, the connections were tested in negative moment and then loaded to a near failure positive moment.

PREVIOUS WORK

The ability of a continuity connection to resist positive moments has been investigated in the United States since the late 1950's when the Portland Cement Association (PCA) published a series of Development Department Bulletins based on half-scale experiments.⁷ Bulletin D43 included the results of seven tests performed on positive moment connections. Three of the connections consisted of welded bars and four consisted of hooked bars. It was concluded that the welded bar connections would perform satisfactorily for both service and ultimate loading conditions. For the hooked bars, which did not perform as well, it was concluded that they would possibly perform satisfactorily provided that some adjustments were made to the detailing of the hooks. It was recommended that the radius of the bend for the hook be increased to at least the diameter of the bar and that the distance from the end of the girder to the inside face of the hook be increased to a minimum of at least twelve times the diameter of the hook bar. Results from this and other bulletins lead to the creation of the 1969 document "Design of Continuous Highway Bridges with Precast, Prestressed Concrete Girders," which is referred to as the PCA Method.² This method is still used by designers throughout the country.

From 1971 to 1974, the Missouri State Highway Commission in cooperation with the Federal Highway Administration investigated the ability to use extended prestressing strands to resist the positive restraint moment.⁸ A total of 69 small scale pullout specimens and 6 full scale connections were tested in order to determine the relationship of the untensioned prestressing strand to the ultimate pullout strength. A relationship for the ultimate stress in the strand at general slip was given as:

$$f_{pu} = \frac{L_e - 8.25}{0.163} \quad (1)$$

where: f_{pu} = ultimate stress in the strand at general slip, ksi
 L_e = embedment length of strand in continuity diaphragm, in.

The National Cooperative Highway Research Program (NCHRP) has sponsored two separate projects addressing continuity in multi-girder bridges. The first study, released as NCHRP Report 322, took place in the mid 1980's and was primarily analytical.⁹ The second study, recently released as NCHRP Report 519, included both analytical and experimental work.⁵

In the NCHRP Report 322, a questionnaire indicated that 18 respondents used embedded bent bars and 21 respondents used extended strands for the positive moment connection, a nearly even 46 to 54 percent split. A FORTRAN based program BRIDGERM (developed in Reference 9) was written to predict the restraint moments that may develop due to secondary effects such as creep and shrinkage of the concrete. A parametric study using the program was performed varying several inputs including the age of the girder when the deck and continuity diaphragm are cast, called the age of continuity. From the parametric study, it was concluded that "...providing positive moment reinforcement has no benefit for flexural behavior of this type of bridge..." and that "...the provisions of positive moment reinforcement at the supports is not recommended." This recommendation was based on two factors. First, the positive moment caused by the positive restraint reinforcing above the

support would cause an increase in the positive mid-span moment, eliminating the benefit of negative continuity. Second, as positive moment develops over a support, cracking would occur in the bottom of the continuity region, requiring sufficient rotation in the section to overcome the cracking before the benefits of negative continuity could be realized.

In the NCHRP Report 519, another questionnaire was developed to determine the state of the practice. This survey confirmed that approximately half of the respondents continue to use extended strands and half use extended bars for the continuity connection. Six full scale stub specimens and two full scale full length specimens were fabricated and tested. It was recommended that the required positive moment capacity of the section should be less than 1.2 times the conventionally calculated cracking moment, M_{cr} . If a design required a capacity greater than $1.2M_{cr}$, then it was recommended that a minimum age of continuity be required in the contract documents to prevent such a high moment from developing. Proposed revisions to the AASHTO LRFD Bridge Design Specifications were made, including the provision to use the equations developed by Salmons⁸ to determine the capacity of a connection with extended prestressing strands. The study also indicated that restraint moments due to thermal effects are significant, with daily temperature fluctuations creating restraint moments as high as 60 percent of M_{cr} . The cost for providing continuity was estimated to be approximately \$200 per girder.

In addition to the conventional cast-in-place continuity diaphragm which relies on the development of the extended strands or bars, alternate types of continuity connections have been proposed and tested. Some connections, such as those developed at the University of Nebraska, make use of threaded rods to connect the tops of the girders to improve the negative moment capacity of the section.¹⁰ The performance of a structure can often be improved by using one of these types of connections. However, due to the limited scope of the project, these types of connections were not considered in this study.

TESTING PROGRAM

OVERVIEW OF TEST SETUPS

Since so many different moments are compared in the testing program, it is important to understand which moment is being discussed. Design moments are the moments which are predicted using the design material properties and a particular design method. The cracking moment, M_{cr} , is a special case of a design moment. In this study, the cracking moment is predicted at the interface of the end of the girder and the continuity diaphragm using the provisions of AASHTO¹¹ modified by the recommendations of NCHRP Report 519.⁵ The cracking moment is taken at this location because this location will produce the lowest positive cracking moment capacity near the continuity diaphragm. It is important that the positive cracking moment within the ends of the girders be designed to have a significantly higher capacity, especially if some strands are debonded. Observed moments are actual moments observed during the testing.

An analytical study was performed to determine the design moments due to secondary effects on a range of different span lengths and slab width arrangements for a two span continuous system. Since the main focus of the study was on the capacity of the continuity connection in positive moment, it was decided to simulate a smaller slab width, since a smaller width will produce less negative (and more positive) restraint moment due to differential shrinkage. For the 28 strand pattern, it was found that an 80 ft (24.4 m) span could be simulated with the given 6 ft (1.8 m) girder spacing. The amount of steel in the deck, 5.58 sq in. (3600 sq mm) was determined to resist the full design negative moment due to superimposed dead load plus live load and impact based on HS 20-44 loading for the test section.

Figure 1 shows the typical test section used for both tests. For each test, two full depth PCBT sections, each 15 ft 4 in. (4.67 m) long and 45 in. (1143 mm) deep were fabricated with different positive moment end connections. For Test 1, the bottom row of 12 - ½ in. (12.7 mm) diameter Grade 270 prestressing strands were extended 24 in. (610 mm) and bent up 9 in. (229 mm) from the ends of the girders. For Test 2, the prestressing strands were cut off flush with the ends of the girders and 4 - No. 6 (19M) Grade 60 hairpin bars were extended 11 in. (279 mm) from the ends of the girders. After fabrication, the girders were transported to the Structures and Materials Laboratory at Virginia Tech where the girders for Test 1 were assembled and the girders for Test 2 were placed in temporary storage.

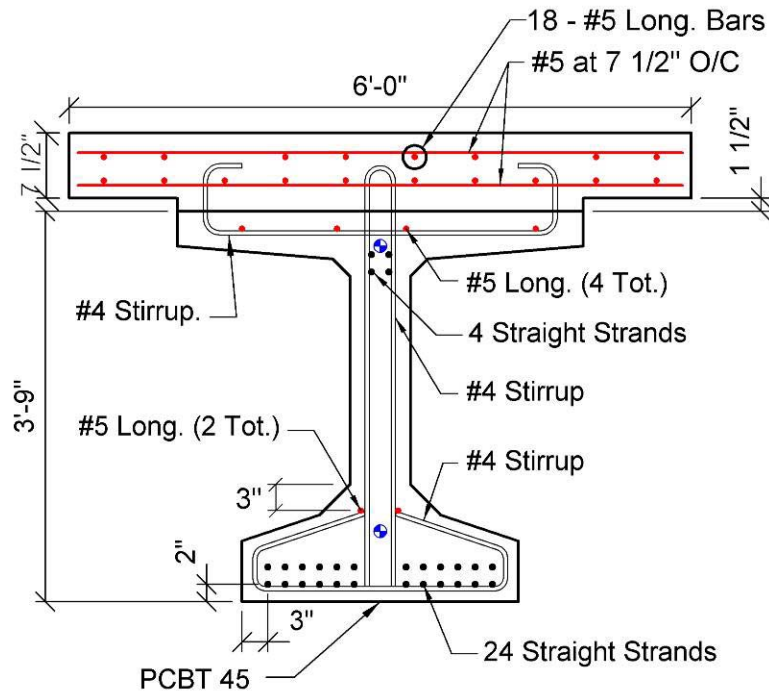
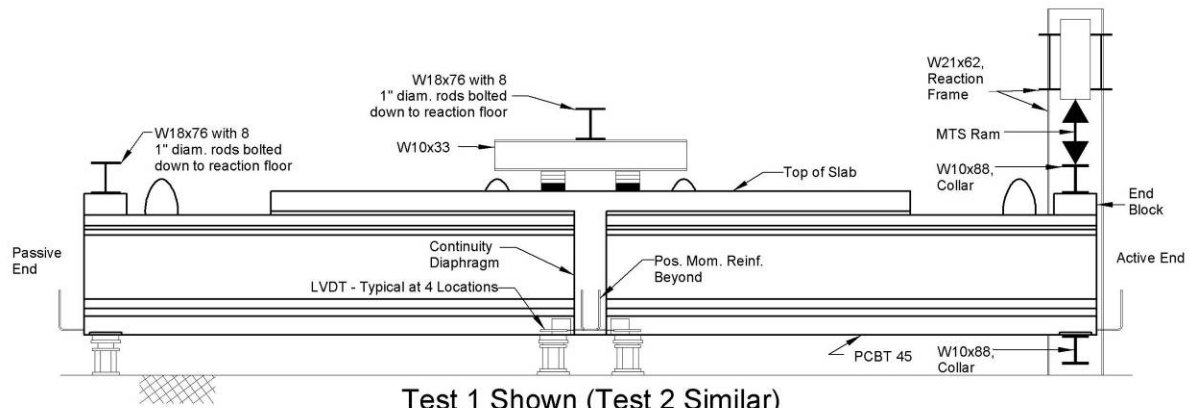


Fig. 1 Typical Test Section

Figure 2 shows a side elevation of the test setup and Figure 3 shows a close-up of one of the LVDTs used to measure the openings at the interface of the end of the girder and the diaphragm. Two girders for Test 1 were set end to end with a gap of 12 in. (305 mm) from



Test 1 Shown (Test 2 Similar)

Fig. 2 Elevation of Test Setup



Fig. 3 Close-up of LVDT

the ends of the girders to produce a two span continuous test setup. The center-to-center bearing length was 14'-0" (4.27 m). Formwork and reinforcing steel were placed to connect the specimens with a reinforced continuity diaphragm and a continuous 6 ft wide (1.83 m) deck. The concrete for the deck and the diaphragm was placed in one pour and was allowed to moist cure for 7 days. The formwork was then removed and the deck concrete was allowed to cure until the target compressive strength of 4,000 psi (27.6 MPa) was reached. Transfer beams were then placed across the top of the specimens at the passive end and the center and bolted down to the reaction floor. The support for the active end was removed and a frame with an MTS actuator was used to support the end with collar beams. This arrangement allowed for the active end of the two span setup to be moved up and down to apply both positive and negative moments at the continuity connection. The test setup for Test 2 was similar, except that the gap at the ends of the girders was 13 in. (330 mm).

Figure 4 shows an overall photo of a test setup for Test 1. The setup for Test 2 was similar. A transfer beam bolted down to the reaction floor is located directly above the continuity diaphragm and the MTS actuator is attached to the far end of the setup with the two collar beams.



Fig. 4 Overall Test Setup

CONNECTION DESIGN

The connections were designed to resist the maximum positive design moment using an easy to construct cast-in-place connection. The 2 in. (50.8 mm) on center pattern for the prestressing strands within the girder was not changed since doing so would result in additional work for the fabricator. For the connection with the extended strands, Test 1, the entire bottom row of 12 prestressing strands were extended and bent up at 90 degrees. For the connection with the extended bars, Test 2, four No. 6 (M19) hairpin bars were placed against the prestressing strands and extended out 11 in. (279 mm). The strands were cut off flush with the end of the girder. Since the recent NCHRP Report 519 did not recommend relying on the embedment of the girder into the diaphragm to provide for an increase in moment resistance, the ends of the girders were designed to be flush with the face of the continuity diaphragms.⁵ For simplicity, the continuity diaphragm and the deck were cast at the same time.

The ultimate positive moment capacity of the connection in Test 1 with the strands was calculated using the allowable ultimate stress in the strands from Equation 1 shown previously. This equation allows the stress in the prestressing strand to reach 98.2 ksi (677 MPa) at ultimate, only 36 percent of its design ultimate strength of 270 ksi (1860 MPa). For Test 2 with the bars, Whitney's equivalent stress block with a phi of 0.9 was used to determine the ultimate positive moment capacity. Figure 5 shows the details of the reinforcing at the continuity connections. The No. 6 (19M) hook bars were designed with the top leg extending 5 ft (1.52 m) into the end of the girder and the bottom leg extending 4 ft (1.22 m) into the end of the girder (based on recommendations in Reference 5). However,

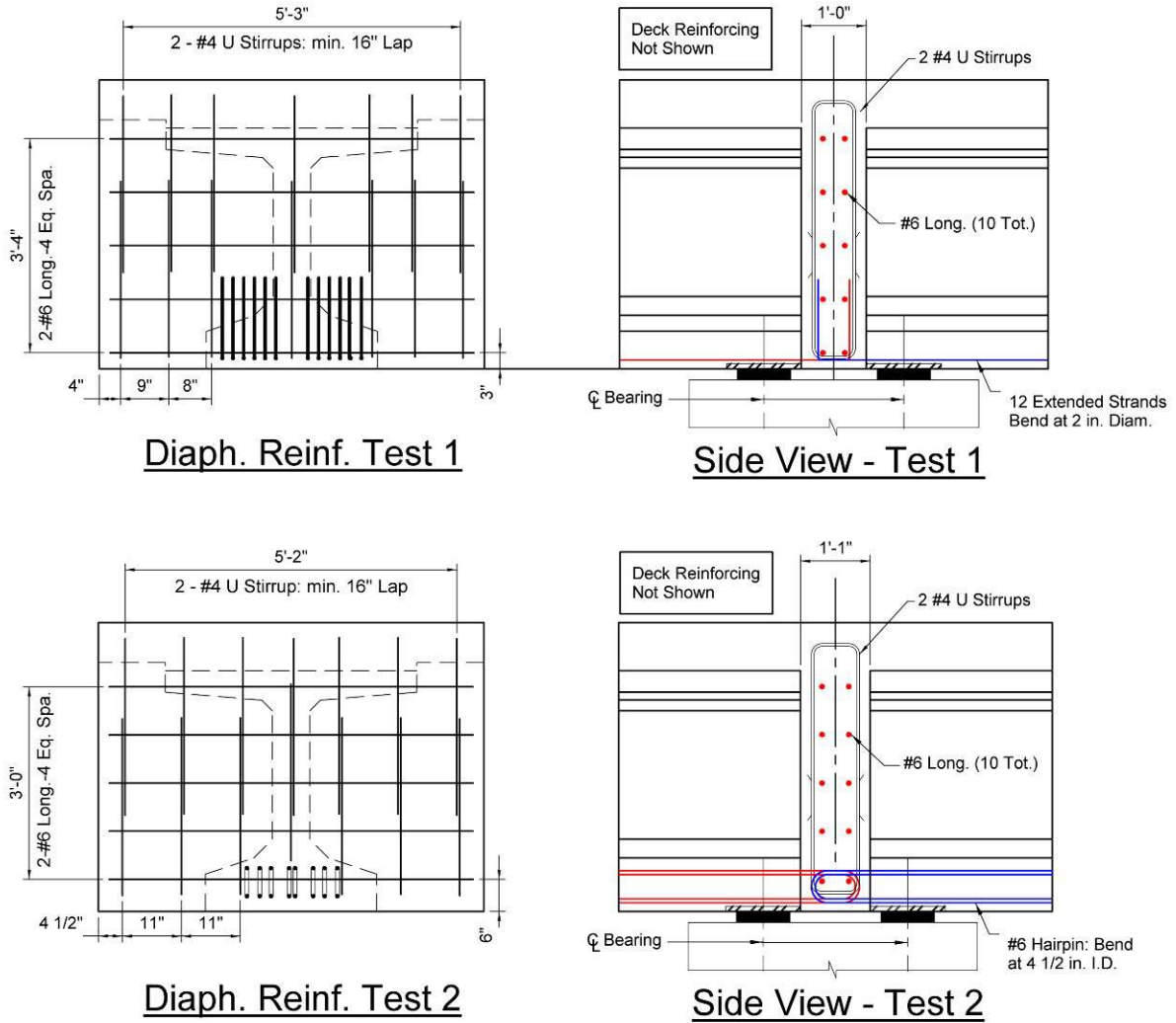


Fig. 5 Details of Continuity Diaphragm Reinforcing

the bars were fabricated with equal length legs, with both the top and bottom legs extending approximately 4 ft (1.22 m) into the end of the girder. Figure 6 shows the extended strands for Test 1 and Figure 7 shows the extended bars for Test 2.

To determine the magnitudes of the design secondary effect moments, the moments due to creep and shrinkage were estimated by averaging the design positive restraint moments from four methods assuming an age of continuity of 28 days.⁴ The design restraint moments due to thermal effects were determined by using the provisions of the AASHTO Guide Specifications¹² and assuming zone three for the solar radiation zone. At the interface of the end of the girder and the continuity diaphragm, the composite section properties were determined using the recommendations of NCHRP Report 519, which recommends using the full cross section at the interface (as shown in Figure 1) and the tensile strength of the diaphragm concrete to determine the design positive cracking moment, M_{cr} .⁵ Table 1



Fig. 6 Extended Strands for Test 1



Fig. 7 Extended Bars for Test 2

Table 1 – Design Properties and Moments

Design Properties	Value
Ultimate Prestressing Strand Strength, f_{pu} (ksi)	270
Ultimate Mild Steel Yield Strength, f_y (ksi)	60
Girder Concrete Compressive Strength at 28 days, f'_c (psi)	8,000
Deck/Diaphragm Concrete Compressive Strength at 28 days, f'_c (psi)	4,000
Girder Gross Moment of Inertia, I_g (in. ⁴)	207,300
Composite Moment of Inertia, I_g (in. ⁴)	451,600
Bottom Distance to Composite Centroid, y_{bot} (in.)	34.1
Top Distance to Composite Centroid, y_{top} (in.)	19.4
Modulus of Rupture for Deck/Diaphragm Concrete at 28 days, f_r (psi)	474
Positive Cracking Moment, M_{cr} (ft-kips)	523
Design Ultimate Positive Moment for Test 1, M_u (ft-kips)	711
Design Ultimate Positive Moment for Test 2, M_u (ft-kips)	773
Design Positive Creep and Shrinkage Moment, M_u (ft-kips)	205
Design Positive Thermal Gradient Moment, M_u (ft-kips)	442

Note: 1 ksi=6.89 MPa; 1 in.=25.4 mm; 1 ft-kip=1.36 kN-m

includes the properties of the girder and the composite section at the interface of the continuity diaphragm as well as the design moments. As shown in Table 1, the Positive Cracking Moment, M_{cr} , is calculated as:

$$M_{cr} = \frac{f_{cr} I_{gc}}{y_{bot}} = \frac{0.474 (451,600)}{34.1(12)} = 523 \text{ ft} - \text{kips} \quad (2)$$

The ultimate design positive moments for the two tests are similar, with Test 2 having approximately 9 percent more capacity than Test 1. For Test 1, with the strands having an allowable stress of 98.2 ksi (677 MPa) as shown earlier, an area of prestressing strands of 12 (0.153 in²) = 1.836 in² (1184 mm²), and a depth to the steel from the top of $d_{ps} = 53$ in. (1346 mm), the Design Ultimate Positive Moment for Test 1, M_u is:

$$a = \frac{A_{ps} f_{ps}}{0.85 f'_c b} = \frac{1.836(98.2)}{0.85(4)72} = 0.736 \text{ in.} \quad (3)$$

$$M_u = \phi \left[A_{ps} f_{ps} \left(d_{ps} - \frac{a}{2} \right) \right] = 0.9 \left[1.836(98.2) \left(53 - \frac{0.736}{2} \right) \right] \frac{1}{12} = 711 \text{ ft} - \text{kips} \quad (4)$$

For Test 2, with the bars having a total area 8 (0.44 in²) = 3.52 in² (2271 mm²), and a depth to the steel from the top of $d_s = 49.25$ in. (1251 mm), the Design Ultimate Positive Moment for Test 2, M_u is:

$$a = \frac{A_s f_y}{0.85 f'_c b} = \frac{3.52(60)}{0.85(4)72} = 0.863 \text{ in.} \quad (5)$$

$$M_u = \phi \left[A_s f_y \left(d_s - \frac{a}{2} \right) \right] = 0.9 \left[3.52(60) \left(49.25 - \frac{0.863}{2} \right) \right] \frac{1}{12} = 773 \text{ ft} - \text{kips} \quad (6)$$

TESTS PERFORMED

Table 2 shows a summary of the tests performed. Since many design procedures consider 1.2 times the design cracking moment, M_{cr} , as a minimum required capacity of the continuity connection, the service tests were designed to apply up to this moment to the sections. The Range column shows the range of the applied positive moment to the continuity diaphragm as a fraction of the design cracking moment. A value of 0, 0.75, 0 indicates that the active end was lifted up using load control to apply zero moment at the continuity connection, then gradually increased up to 0.75 times the cracking moment, M_{cr} , then gradually decreased back to zero moment. Tests A through C were done to investigate the initial service characteristics of the connections. Following the service testing, Tests D through J were done to simulate the application of cyclic positive and negative thermal restraint moments.

Table 2 – Tests Performed

Test Name	Range, % Mcr	Number of Cycles
1A	0 , 0.75 , 0	0
1B	0 , 1.0 , 0	0
1C	0 , 1.20 , 0	0
1D	0 , 1.0 , 0	1,000
1E	0 , 1.0 , 0	2,000
1F	0 , 1.0 , 0	2,000
1G	0 , 1.0 , 0	2,000
1H	0 , 1.0 , 0	2,000
1J	0 , 1.0 , 0	1,000
1K	0,1,0,-1,0	0
1L	0,1,0,-1,0,1,0,-1,0	0
1M	0,1,0,-1,0,1.7,0	0
1N	0 , 1.83 , 0	0
2A	0 , 0.75 , 0	0
2B	0 , 1.0 , 0	0
2C	0 , 1.20 , 0	0
2D	0 , 1.0 , 0	1,000
2E	0 , 1.0 , 0	2,000
2F	0 , 1.0 , 0	2,000
2G	0 , 1.0 , 0	2,000
2H	0 , 1.0 , 0	2,000
2J	0 , 1.0 , 0	1,000
2K	0,1,0,-1,0	0
2L	0,1,0,-1,0,1,0,-1,0	0
2M	0 , 2.07 , 0	0

The cyclic loads were applied at a rate of 0.25 Hertz and were designed to simulate the total number of full thermal cycles a structure may encounter over its design service life. The applied thermal moments ranged from a positive moment of 442 ft-kips (599 kN-m) to a negative moment of -105 ft-kips (-142 kN-m). The magnitudes of the cyclic loads were gradually increased as a fraction of the full thermal moments from 0.25, 0.5, 0.75, to 1.0 for Tests D, E, F, and G respectively. The full thermal moments were also used for Tests H and J. Following the cyclic testing, negative moment and ultimate positive moment tests were performed.

SERVICE TEST RESULTS

The results of the service tests, Tests A through C, for both Test 1 and Test 2 are shown in Fig. 8 at the same scale so that an easy comparison can be made. The moment applied to the continuity diaphragm as a fraction of the design cracking moment, M_{cr} , is plotted on the vertical axis and the average measured LVDT reading at the bottom of the interface of the continuity diaphragm and the end of the girder is plotted along the horizontal axis. Four LVDTs, one at each of the four corners, were placed near the bottom of the interface to measure the crack openings at those locations (see Figure 3). The magnitudes of the crack openings at the four locations were similar, so the results are presented as an average of the four values. The LVDT readings compared well with visually observed measurements of the crack openings using both a crack comparator card and dial gages.

The initial visual cracking at the bottom of the interface occurred at approximately $0.41 M_{cr}$ (215 ft-kips or 292 kN-m) for Test 1 and $0.45 M_{cr}$ (236 ft-kips or 320 kN-m) for Test 2, both much lower than the design cracking moment $1.0 M_{cr}$ of 523 ft-kips (709 kN-m). This behavior was not unexpected, since the interface at the end of the girder acts as a cold joint, the cracking that occurred can be considered as debonding of the diaphragm concrete from the end of the girder. Even though the cracking is not desirable at such a low moment, the cracking or debonding was well defined along the interface, allowing for possible easy mitigation.

At the age of the decks for the initial service tests, 35 days for Test 1 and 23 days for Test 2, the compressive strength of the deck/diaphragm concrete was approximately 1.45 times the design 28 day strength of 4,000 psi (27.6 MPa). Using the actual compressive strength of the diaphragm concrete at the time the initial cracking occurred, a better prediction of the tensile capacity of the concrete at the interface was developed. Using a prediction for the tensile capacity of the concrete across the interface equal to $(1/4)(w f_c)^{(1/2)}$ where w is the unit weight of the concrete in pounds per cubic foot and f_c is the compressive strength in psi gives a predicted moment at initial cracking of approximately 253 ft-kips (343 kN-m), which is much closer to the observed values.

Based on the shapes of the responses to the initial tests shown in Figure 8, the two tests show similar responses to the initial service tests. However, Test 2 with the extended bars exhibited slightly smaller crack openings at the bottom of the interface than Test 1. The ratio of the design ultimate positive moment of Test 1 to Test 2 was 0.92, while the observed ratio of the average LVDT reading of Test 1 to Test 2 was 1.32, indicating that based on the design ultimate positive moments, Test 2 displayed a stiffer response to the initial service tests.

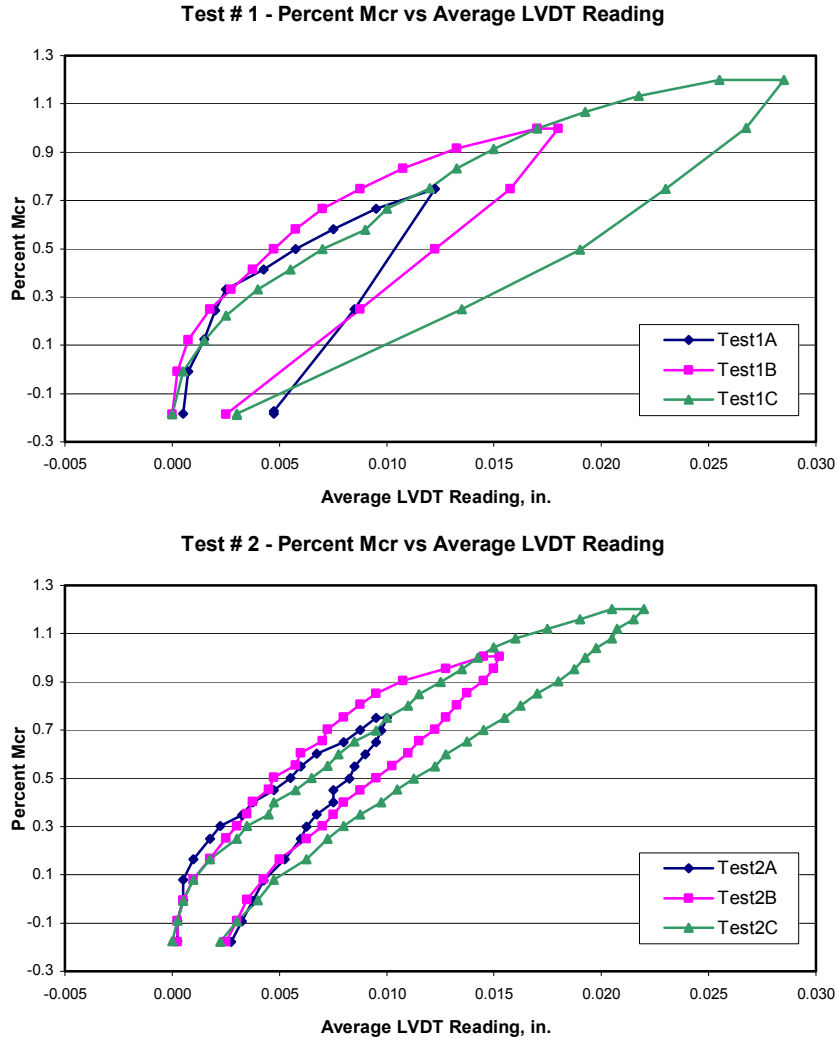


Fig. 8 Service Test Results

CYCLIC TEST RESULTS

The results of the cyclic tests, Tests D through J, for both Test 1 and Test 2 are shown in Figure 9 at the same scale so that an easy comparison can be made. The two span specimens were initially subjected to an active end load that would cause a zero applied moment at the continuity connection in order to zero all of the instrumentation. A set of measurements was taken, the cyclic loads were applied, and then the specimens were tested up to 1.0 times the design positive cracking moment, M_{cr} . The percent of the cracking moment applied is shown on the vertical axis and the average measured LVDT reading is shown on the horizontal axis. The cyclic loads included both positive and negative moments, but the loading for the response shown in the figure was done only in the positive moment range in order to match Tests A through C.

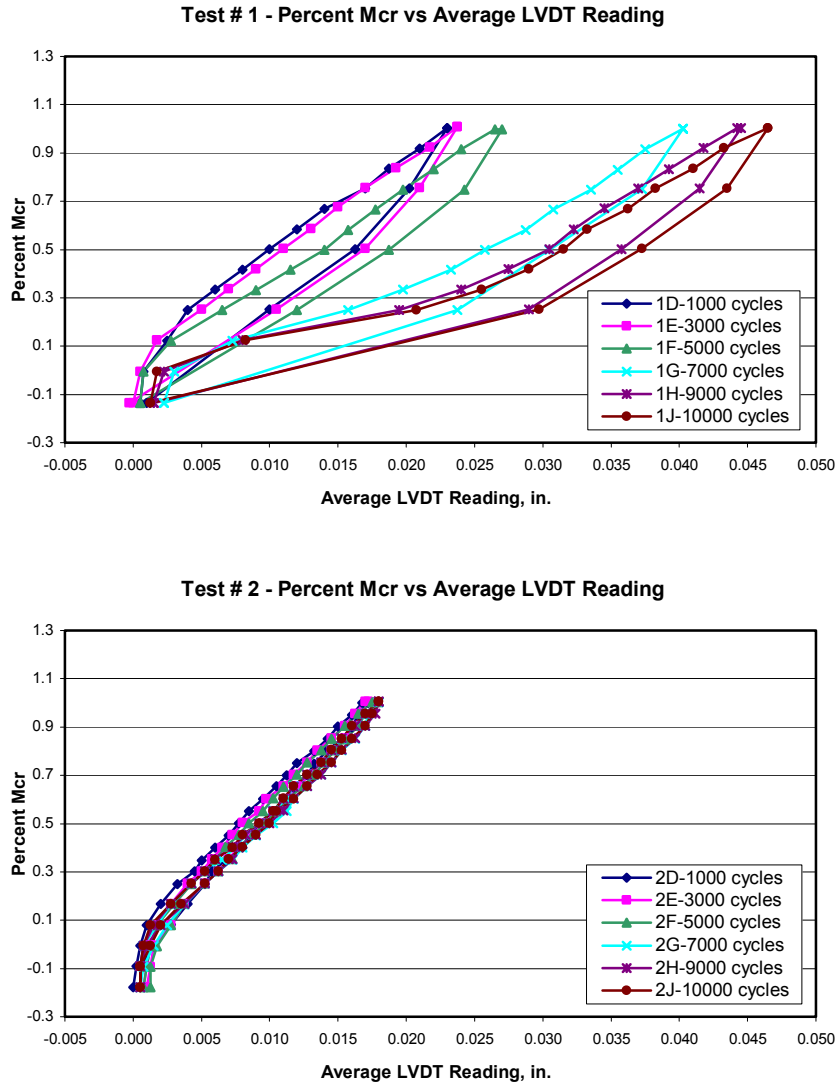


Fig. 9 Cyclic Test Results

Both tests maintained integrity throughout the cyclic loading phase and were able to withstand the applied moment of 1.0 times the cracking moment even after being subjected to 10,000 cycles. However, by comparing the responses, it is apparent that Test 2 with the bars performed better than Test 1 with the strands. After application of the 10,000 cycles, Test 1 displayed an average LVDT opening of 0.047 in. (1.19 mm) while Test 2 displayed an average LVDT opening of only 0.018 in. (0.46 mm), approximately 2.6 times less opening at the interface. Therefore, under cyclic loads, Test 2 remained stiffer than Test 1.

The response of Test 2 to the cyclic loads remained virtually unchanged throughout the testing. However, the response of Test 1 did change significantly. As Salmons reported, untensioned prestressing strands have been observed to develop a tendency to slip when

pulled in tension.⁸ It is believed that as the untensioned strands in the diaphragm are pulled, the wires have a tendency to twist and locally unwind through the surrounding concrete. For a pretensioned strand, Hoyer's effect acts to counteract the loss in development due to the twisting action. However, for the strands in the diaphragm which are not pretensioned, it is believed that the strands developed a lower bond throughout the applied cycles because of the unwinding of the strands from the location of the interface to the 90 degree bend and localized concrete damage. This lower bond allowed the magnitude of the cracking as measured by the LVDT readings to increase.

Figure 10 shows average measured LVDT reading on the vertical axis plotted against the number of cycles shown on a log scale on the horizontal axis. Test 2 shows desirable behavior, with a slight, linear increase in the average measured LVDT reading throughout the 10,000 cycles. Test 1 shows undesirable behavior beginning at approximately 5,000 cycles, with a significant increase in the average measured LVDT reading.

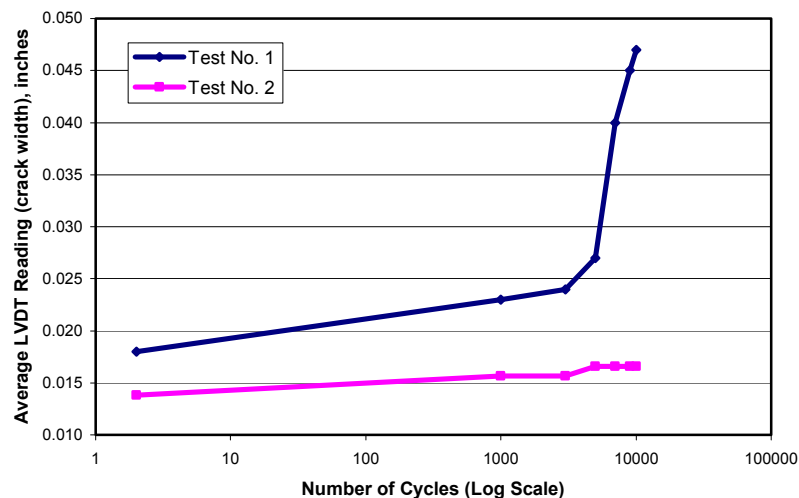


Fig. 10 Average LVDT Reading versus Number of Cycles

There was no noticeable cracking in the girders for Test 1 with the strands. For Test 2, some minor cracking in the girders near the bottom of the web along the top of the bottom flange occurred during the cyclic loading after the 9,000th cycle. The cracking was minor, and never exceeded 0.002 in. (0.050 mm) in width or extended more than 19 in. (480 mm) into the girder. The cracking was most likely due to the bursting forces created by the bars in tension. Although any cracking in the girders is undesirable, the cracking was minor in both width and length, and is not expected to pose a significant problem.

NEGATIVE MOMENT TESTING

The purpose of the negative moment testing was to confirm the repeatability of the response of the two span systems after being subjected to the full design negative cracking moment.

Figure 11 shows Test L for both Test 1 and Test 2. Both tests were performed by first applying a positive cracking moment and then applying a negative cracking moment. Two complete load cycles were performed for each test, the first cycle designated “A” and the second cycle designated “B”. Both tests display good repeatability from the first cycle to the second. Test 1 continued to display a response indicating that the strands were twisting through the diaphragm concrete until the 90 degree bend is engaged. Test 2 displays a nearly linear response in both the positive and negative moment directions.

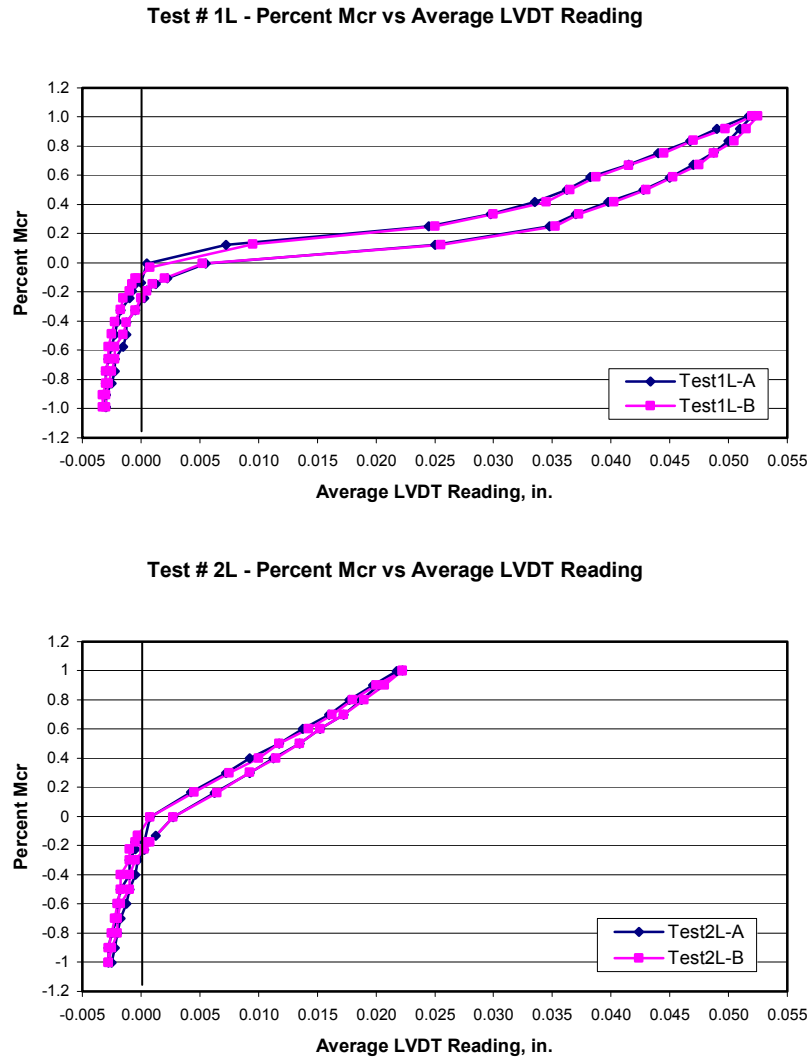


Fig. 11 Negative Moment Testing Results

ULTIMATE STRENGTH RESULTS

The purpose of the ultimate strength testing was to confirm the design ultimate positive moments could be obtained even after the cyclic loading. Both tests were taken to a near failure positive moment by increasing the active end deflection and monitoring the applied load. Figure 12 shows the results for both Test 1 and Test 2, with the applied moment on the vertical axis and the observed active end deflection along the horizontal axis.

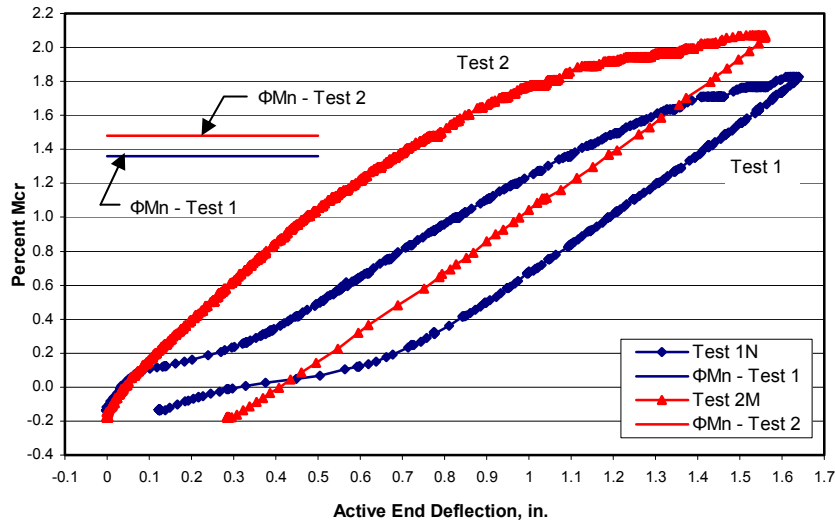


Fig. 12 Ultimate Strength Test Results

For safety reasons, the bottom of the diaphragm could not be monitored continuously during the test. However, it was inspected periodically in order to determine when first cracking occurred in the bottom of the diaphragm. For consistency, the capacities are presented as a fraction of the design positive cracking moment, 523 ft-kips (709 kN-m). For Test 1, first cracking was noticed at an applied moment of $1.4M_{cr}$, and for Test 2, first cracking was noticed at an applied moment of $1.2M_{cr}$. Both tests reached and exceeded the design ultimate positive moments. For Test 1, the observed capacity approached slightly over $1.8M_{cr}$ while the design ultimate moment, ϕM_n , was $1.36M_{cr}$. For Test 2, the observed capacity approached slightly over $2.0M_{cr}$ while the design ultimate moment, ϕM_n , was $1.48M_{cr}$. The ratio of the observed to design moments was 1.32 for Test 1 and 1.35 for Test 2. Therefore, both design methods for predicting the design ultimate positive moments provided conservative estimates, over predicting the capacities by factors of 1.32 and 1.35, respectively.

Significant cracking occurred on the bottom of the continuity diaphragms for both tests near the ultimate loads, indicating that both the strands and the bars were able to transfer tensile forces well beyond the forces required to be transferred for service loads. The cracking on the bottom of the diaphragm was limited to a region confined within the width of the bottom flange of the girders, also indicating that the transfer of load within the connection occurred primarily within the width of the bottom flange of the girder.

CONCLUSIONS

The observed initial positive cracking moment at the interface of the end of the girder and the continuity diaphragm was lower for both tests than predicted assuming a tensile capacity equal to the modulus of rupture of the diaphragm concrete. A better predictor for the initial tensile capacity of the concrete at the interface is recommended. However, even though cracking occurred earlier than predicted, the cracking was well defined, and the connections for both tests were able to resist positive moments up to 1.2 times the design cracking moment, M_{cr} , during the initial service testing. Test 2 with the extended bars displayed a slightly stiffer response to the applied moments when compared to Test 1 with the extended strands. The crack openings at the bottom of the connection were approximately 1.3 times larger for Test 1 than Test 2 at the end of the service testing.

Throughout the cyclic testing, both test sections were capable of resisting the applied cyclic thermal moments and the test moments up to 1.0 times the design cracking moment, M_{cr} , which were applied after the application of the cyclic moments. But, during the cyclic testing, Test 1 began to display some undesirable behavior as the crack openings began to increase at approximately the 5,000th cycle and continue to increase until the end of testing. At the end of the cyclic testing, crack openings for Test 1 were 2.6 times larger than the crack openings for Test 2. Therefore, the connection with the extended bars, Test 2, remained stiffer throughout the cyclic testing.

Both test connections showed good repeatability during the negative moment testing phase. Even after the application of 10,000 positive and negative moment cycles, the sections were able to reliably withstand the application of a positive moment up to 1.0 times the cracking moment, M_{cr} .

Both Test 1 and Test 2 exceeded the design ultimate positive moments by ratios of 1.32 and 1.35, respectively. The design ultimate positive moments using the method proposed by Salmons⁸ for Test 1 and conventional Whitney's equivalent stress distribution with a phi of 0.9 for Test 2 conservatively predicted the observed ultimate positive moments.

For both tests, the ends of the girders were designed to be flush with the continuity diaphragm. It is believed that this detail enabled the cracking at the interface of the end of the girder and the continuity diaphragm to remain well defined throughout the service tests. This well defined cracking could be mitigated at initial construction by application of a material able to withstand movements conservatively up to approximately 0.05 in. (1.3 mm). Since embedding the ends of the girder into the continuity diaphragm is not believed to increase the capacity significantly, and will result in more cracking and spalling at the interface, it is recommended to detail the ends of the girder flush with the end of the continuity diaphragm to force all service load level damage across the cold joint.

The connection with the extended 180 degree bent bars is recommended for use in typical design situations. Although the connection cracks at the interface under positive moment

prior to reaching 1.2 times the design cracking moment, it is able to resist moments well beyond this value in a cracked state. Throughout the cyclic testing, the connection remained stiffer than the connection with the extended strands. Also, the connection displayed sufficient strength for the design ultimate positive moment. Even though the ends of the bars were not staggered vertically due to a fabrication error, it is recommended to follow the provisions of NCHRP Report 519 when detailing the embedment lengths of the bars.⁵ In all cases, the bars should extend well into the fully prestressed portion of the beam.

ACKNOWLEDGMENT

The research presented was sponsored by the Virginia Department of Transportation and the Virginia Transportation Research Council. The contents do not necessarily reflect the official views or policies of the Virginia Department of Transportation. The authors would like to thank the sponsors for funding this much needed research.

REFERENCES

1. Kaar, P.H., Ladislav, B.K., and Hognestad, E., "Precast-Prestressed Concrete Bridges. 1. Pilot Tests of Continuous Bridges. Development Department Bulletin D34." Portland Cement Association, Research and Development Laboratories, Skokie, Illinois, 1960.
2. Freyermuth, C.L., "Design of Continuous Highway Bridges with Precast, Prestressed Concrete Girders." *Journal of the Prestressed Concrete Institute*, Vol. 14, No. 2, 1969. Also reprinted as PCA Engineering Bulletin (EB014.01E), Portland Cement Association.
3. McDonagh, M. D., Hinkley, K. B., "Resolving Restraint Moments: Designing for Continuity in Precast Prestressed Concrete Girder Bridges", *PCI Journal*. v 48 n 4 July/August 2003. pgs. 104-119.
4. Newhouse, C.D., Roberts-Wollmann, C.L., and Cousins, T.E., "Influences of Design Methods and Assumptions on Continuity Moments in Multi-Girder Bridges", PCI National Bridge Conference, Oct. 17-20, 2004, Atlanta, Ga.
5. Miller, R.A., Castrodale, R., Mirmiran, A., Hastak, M., "Connection of Simple-Span Precast Concrete Girders for Continuity," Transportation Research Board's National Cooperative Highway Research Program, NCHRP Report 519, 2004.
6. Hastak, M., Mirmiran, A., Miller, R., Shah, R., and Castrodale, R., "State of Practice for Positive Moment Connections in Prestressed Concrete Girders Made Continuous," *Journal of Bridge Engineering*, ASCE, September/October 2003.
7. Mattock, A.H., Kaar, P.H. "Precast-Prestressed Concrete Bridges 3. Further Tests of Continuous Girders. Development Department Bulletin D43." Portland Cement Association, Research and Development Laboratories, Skokie, Illinois, 1960.
8. Salmons, J.R., "End Connections of Pretensioned I-Beam Bridges", Missouri Cooperative Highway Report 73-5C, Missouri State Highway Department, Jefferson City, Missouri, 1974.

9. Oesterle, R.G., Glikin, J.D., and Larson, S.C., “Design of Precast Prestressed Girders Made Continuous”, National Cooperative Highway Research Program Report 322, National Research Council, Washington, D.C., 1989.
10. Saleh, M. A., Einea, A., and Tadros, M. K., “Creating Continuity in Precast Girder Bridges,” *Concrete International*, August 1995.
11. American Association of State Highway and Transportation Officials (AASHTO), *Standard Specifications for Highway Bridges – 17th Edition – 2002*, Washington, D.C.
12. American Association of State Highway and Transportation Officials (AASHTO), *AASHTO Guide Specifications – Thermal Effects in Concrete Bridge Superstructures – 1989*, Washington, D.C.